Supplementary content associated with Fonseca et al. (2026). Advances in Geochemistry and Cosmochemistry, 2(1), 754. https://doi.org/10.33063/agc.v2i1.754

Supplementary material: The case for metal saturation in the lunar mantle (2026-06-03)

Raúl O. C. Fonseca[1], Christopher Beyer[1], Stephan Schuth[1], Felipe P. Leitzke[2]
[1] Institut für Geologie, Mineralogie und Geophysik, Ruhr-Universität Bochum
[2] Universidade Federal the Pelotas, Pelotas, Rio Grande do Sul, Brasil
Correspondence to: Corresponding Author, raul.fonseca@rub.de

Online supplementary material: https://doi.org/10.5281/zenodo.14966151

Supplementary Figures

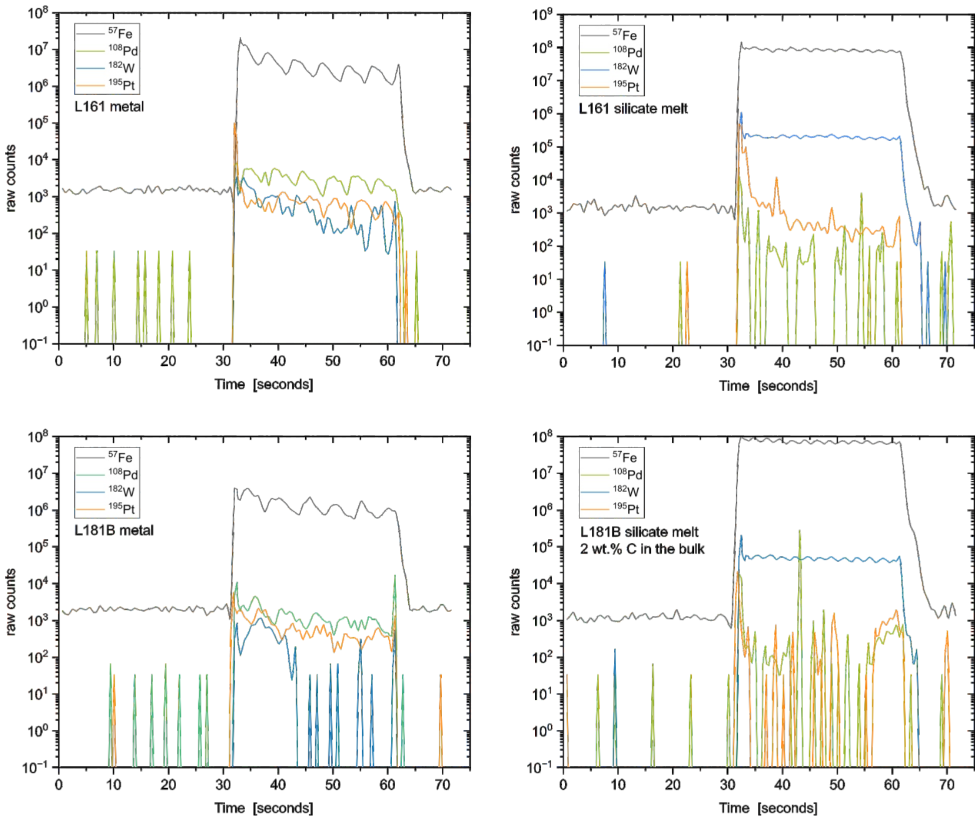

Figure S1: Examples of the LA-ICP-MS transient signal in our experiments. The first column exemplifies a typical signal for the Fe-S metal in our experiments for C-free (L161) and C-bearing experiments. A comparison between the signal for the quenched silicate glass in the same samples (2nd column) highlights how "noisier" the transient signal for the C-bearing experiment is compared to the C-free experiment, potentially indicating a higher proportion of nanonuggets in the former compared to the latter.

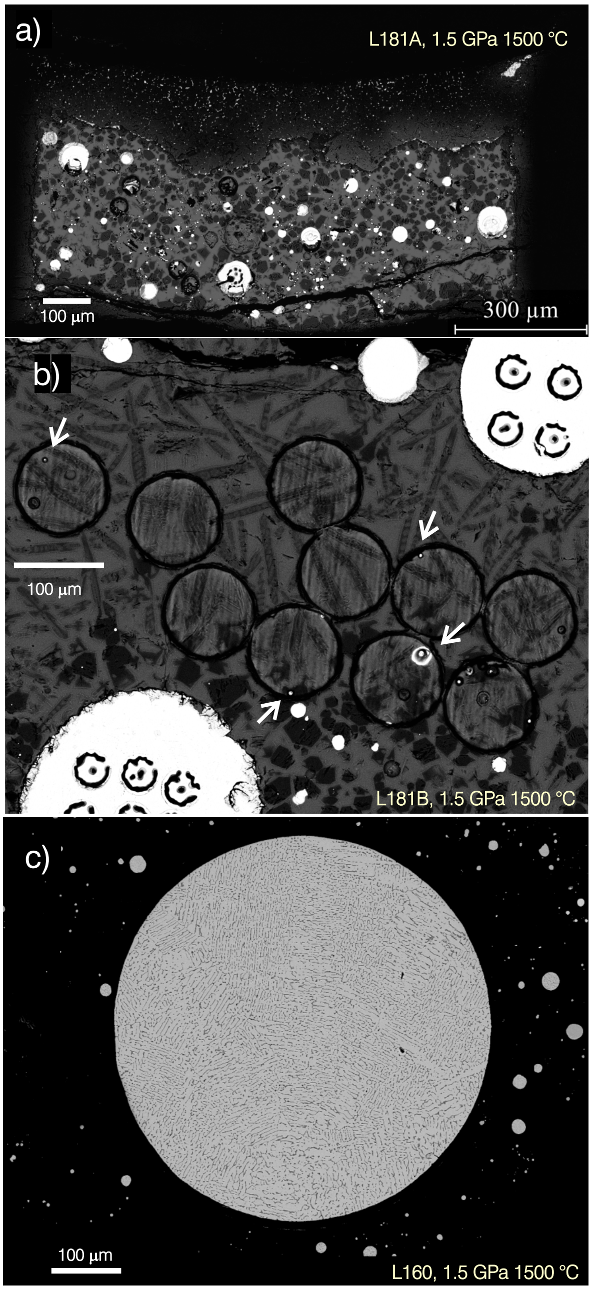

Figure S2: Further examples of typical experimental run products shown in a backscatter electron (BSE) image. a) Overview of C-bearing experiment L181A, which was present in the colder end of a multi capsule piston cylinder assembly, and does displayed a large degree of crystallization. Nugget contamination during LA-ICP-MS analysis was unavoidable resulting in lower $D_i^{met/sil}$ for most siderophile elements. b) Higher magnification BSE image of C-bearing experiment L181B, where the white arrows indicate where laser spots are shown to have included metal nuggets during the LA-ICP-MS analysis. c) Contrast enhanced BSE image showing the typical quench texture of the liquid metal blebs in experiment L160.

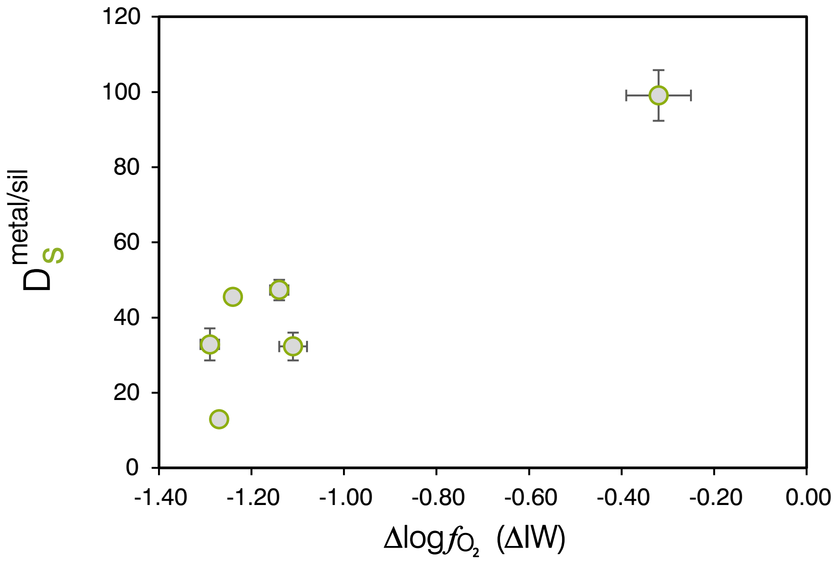

Figure S3: Broad positive correlation between the metal/silicate partition coefficient for S, and log fO_2 (relative to the IW reference redox reaction). This correlation is constrained by a single experiment carried out at IW-0.32 (L162), which is also the one with the highest S content in metal (21.8 wt.%).

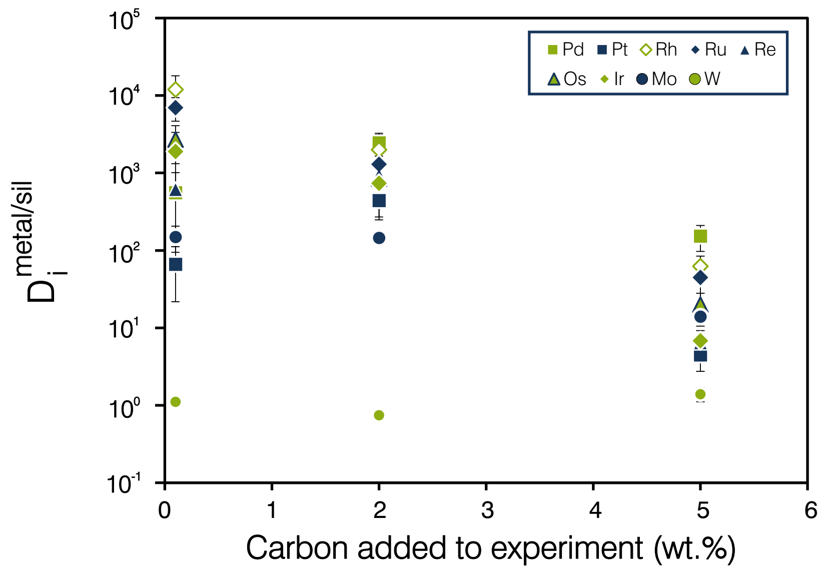

Figure S4: Relationship between $D_i^{metal/sil}$ and the carbon content added to experiments (Series L181A-C). Except for W, partition coefficients are all lower with increasing C content added to the experiments. However, it is hard to know whether this represents actual equilibrium concentrations or simply a higher nanonugget content in the silicate glass at higher C contents. Experiment L181A, which had no C added, was also the one with the highest degree of crystallization, owing to it sitting in the cold end of a multi-capsule piston cylinder assembly. The higher crystallization degree resulted in a much larger scatter in the measured elemental concentrations due to unavoidable contamination during LA-ICP-MS measurements.

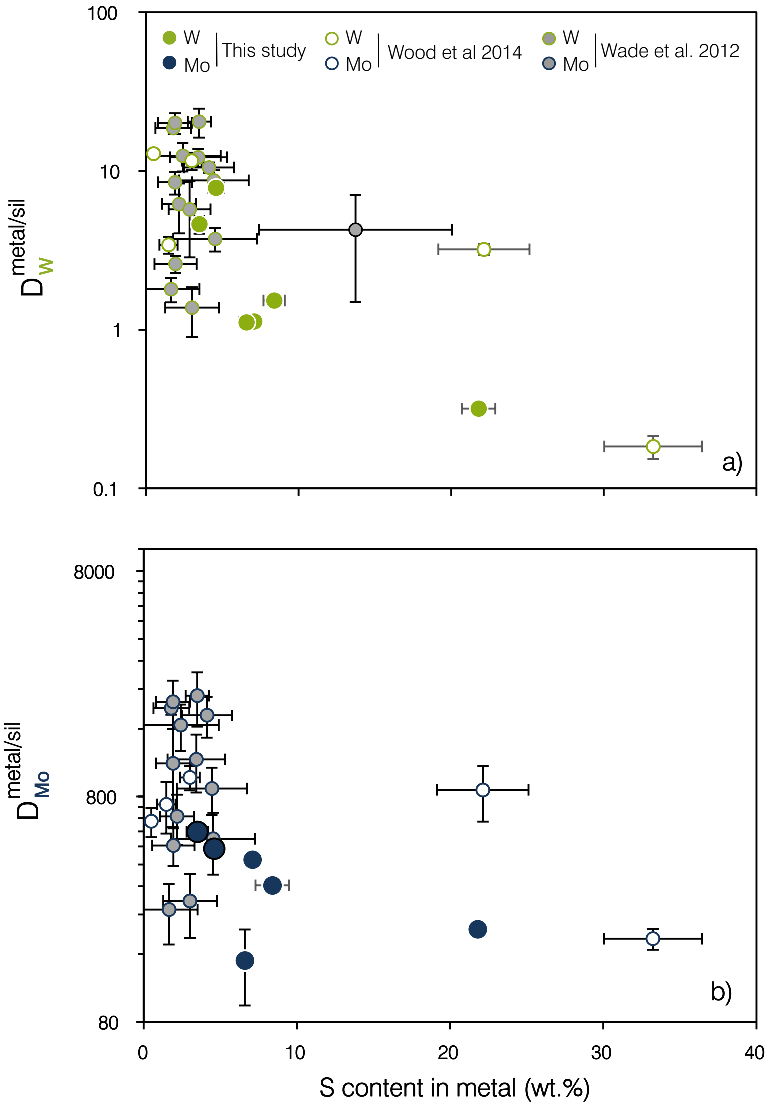

Figure S5: Comparison between our partitioning data for W (a) and Mo (b) and literature data from Wood et al. (2014) and Wade et al. (2012). The Wade et al. (2012) comprises experimental results pertaining to compositions where the degree of melt polymerization and silica activity were changed, and the role of S was not, strictly speaking, a main factor in these experiments. This is exemplified by the fact that most $D_{Mo,W}^{metal/sil}$ in Wade et al. (2012) cluster at low S contents in metal (less than 5 wt.%), and spread over a factor of roughly ten.

References

Wade, J., Wood, B. J. and Tuff, J. (2012). Metal–silicate partitioning of Mo and W at high pressures and temperatures: evidence for late accretion of sulphur to the Earth. *Geochimica et Cosmochimica Acta* 85: 58–74.

Wood, B. J., Kiseeva, E. S. and Mirolo, F. J. (2014). Accretion and core formation: the effects of sulfur on metal–silicate partition coefficients. *Geochim. Cosmochim. Acta* 145: 248–267.